SLAC-PUB-12287
January 2007

Active RF Pulse Compression Using Electrically Controlled Semiconductor Switch

Jiquan Guo, Sami Tantawi
SLAC, Stanford University, 2575 Sand Hill Rd, Menlo Park, CA 94025

Abstract: First we review the theory of active pulse compression systems using resonant delay lines. Then we describe the design of an electrically controlled semiconductor active switch. The switch comprises an active window and an overmoded waveguide three-port network. The active window is based on a four-inch silicon wafer which has 960 PIN diodes. These are spatially combined in an overmoded waveguide. We describe the philosophy and design methodology for the three-port network and the active window. We then present the results of using this device to compress 11.4 GHz RF signals with high compression ratios. We show how the system can be used with amplifier like sources, in which one can change the phase of the source by manipulating the input to the source. We also show how the active switch can be used to compress a pulse from an oscillator like sources, which is not possible with passive pulse compression systems.

I. INTRODUCTION

RF pulse compression systems and their application to RF accelerator systems was first introduce by Z. Farkas and P. Wilson through the invention of the SLED pulse compression system[1]. This system produced a non-flat rf output and was suitable basically for single bunch acceleration. It resulted in almost doubling the SLAC linac energy and was one of the enabling technologies for building the Stanford Linear Collider (SLC). The main reason that pulse compression system was so successful is that it matches the requirement of RF accelerator structures of high power short pulses to the naturally produced lower power long pulses from most RF microwave tubes.

RF pulse compression was researched extensively during the last two decades because of the desire to build the next generation of linear colliders. Several of these collider designs were based on multi-bunch acceleration, which in turn needed and RF system that can produce a flat top RF signal. One such system is the Binary Pulse Compression system (BPC) [2]. This system is extremely efficient and produces flat top output pulses. However, it comprises a cumbersome set of overmoded waveguides, which act as a low-loss delay lines. To make this system more compact resonant delay pulse compression system was invented by Wilson et. al [3] and Fiebig et. el [4] independently. This system is much more compact than the BPC system but it suffer from a reduced intrinsic efficiency. The efficiency of resonant delay lines deteriorates very fast with high compression ratios and it has a theoretical maximum power gain of 9 for lossless systems.

To improve the efficiency of the resonant delay line pulse compression system, active pulse compression systems have been suggested [5]. The theory of active pulse compression was introduced also in [5]; we will briefly review this theory. These systems require a switch with low insertion loss, fast switching time and high power handling capacity. Ferromagnetic [6], ferroelectric [7], and plasma [8] switches have been suggested as possible candidates for the switch. A switch based on bulk effects in

Submitted to New J.Phys.
Work supported by the US Department of Energy contract DE-AC02-76SF00515

semiconductors has been demonstrated. This switch is based on the excitation of electron hole plasma on the surface of a semiconductor using a 100mJ 5ns laser pulse [9]. To eliminate the laser from the system described in [9], PIN diode junctions have been used to inject the carriers into the bulk of a semiconductor wafer [10].

Discrete component PIN diodes have been used as microwave switches for more than half a century and are still widely used. The diode has an undoped region (also called intrinsic region, or I region) between two heavily doped P and N regions. The switching time for a discrete PIN diode is determined by the time needed for the electrons/holes to sweep through the intrinsic region, which is typically several nanoseconds. Although discrete component PIN diodes have high RF power handling capacity compared to many other discrete component RF switches, they are still far away from the targeted application of pulse compression systems for high energy accelerator structures which requires the handling of tens of megawatt RF power. In the 1960's, the idea of waveguide window switch was suggested, and several switches were developed [13, 14]. The window switch comprises a high resistivity silicon wafer integrated with a set of PIN diodes. When the switch is inserted into the waveguide, the PIN diodes can inject carriers into the bulk silicon to form conductive plasma and switch the RF reflectivity. Such a switch was developed in rectangular waveguides, and was tested up to 100kW power level at X-band. The power level is mainly limited by the choke structure, which is employed to avoid the RF leakage at the gap where the window switch is inserted.

The switch window proposed in [10] operates under the TE_{01} mode in a circular waveguide. This mode has no radial electric field and no azimuthal magnetic field; hence, a small gap in the waveguide will not lead to RF leakage without the choke structure. The switch was able to handle multi-megawatts of RF power. Ref [10] also details the scaling laws for combining a set of these switches. However, the device described in [10] demonstrated only the possibility of the use of such technology with ultra-high power microwave systems. This device was too slow for pulse compression application and had high losses; it lacked all the necessary ingredient for practical application into pulse compression system.

Here, we present a design for such a switch based on injecting the carrier at the surface of a silicon wafer using an array of 960 PIN surface diodes. This switch is fast enough and its losses are low enough for pulse compression applications. The process for the PIN diodes is compatible with the popular CMOS IC process, so the unit cost should be moderate if it's produced in volume. The requirement of the driver for the solid state silicon switch is also lower than other options. A typical setup uses a 1kV 1kA pulsed power driver, while the plasma switches and the ferroelectric switches need about 100KV driver voltage, and the optical switch requires a costly high-power laser.

The wafer with its array of PIN diodes represents an active window. This window operates at the TE_{01} mode in circular waveguide, i.e; the array is spatially combined in an overmoded waveguide. The choice of the TE_{01} mode enable use to insert the active window in the waveguide because it does not have any axial currents. Because the switch used in the pulse compression system application is required to change its reflection coefficient between two preset states which are neither one nor zero, we used a three port network to transfer the natural two states of the switch, namely completely transmissive or completely reflective, to the two required states needed by the pulse compression system. The three-port network is an overmoded device with all its ports operating at the

TE_{01} mode. In the following part of this paper, we describe the design of such a switching system. We also demonstrate it by using it into a resonance delay line pulse compression system. We show how the system can be used with amplifier like sources, in which one can change the phase of the source by manipulating the input to the source. We also show how the active switch can be used to compress a pulse from an oscillator like sources, which is not possible with passive pulse compression systems.

II. THEORY OF ACTIVE RESONANT DELAY LINE PULSE COMPRESSION SYSTEM

The theory of active pulse compression with several time events is detailed in [5]. Here, we describe the special case of a *single event* switched pulse compression system.

Figure 1. Resonant delay line.

Consider the waveguide delay line with a coupling iris shown in Fig. 1. The *lossless* scattering matrix representing the iris is unitary. With proper choice of reference planes the matrix takes the following form:

$$\underline{\underline{S}} = \begin{pmatrix} -R_0 & -j(1-R_0^2)^{1/2} \\ -j(1-R_0^2)^{1/2} & -R_0 \end{pmatrix}. \qquad (1)$$

R_0 is the reflection coefficient of the iris. In writing Eq. (1) we assumed a symmetrical structure for the iris two-port network. The forward and reflected fields around the iris are related as follows:

$$V_1^- = -R_0 V_1^+ - j(1-R_0^2)^{1/2} V_2^+, \qquad (2)$$

$$V_2^- = -j(1-R_0^2)^{1/2} V_1^+ - R_0 V_2^+. \qquad (3)$$

With the exception of some phase change, the incoming signal V_2^+ at time instant t is the same as the outgoing signal V_2^- at time instant $t - \tau$, where τ is obviously the round trip delay through the line; i.e.

$$V_2^+(t) = V_2^-(t-\tau)e^{-j2\beta l}.; \qquad (4)$$

where β is the wave propagation constant within the delay line, and l is the length of the line. Substituting from Eq. (4) into Eq. (3) we get a difference equation that governs the system. During the charging phase we assume a constant input V_{in}. If the delay line has small losses (β has a small imaginary part), at resonance the term $e^{-j2\beta l} = -p.$ where p is a positive real number close to 1. We, also, assume that all the voltages are equal to zero at time $t < 0$. After the energy has been stored in the line one may dump part of the energy in a time interval τ by flipping the phase (changing it suddenly by π) of the

incoming signal just after a time interval $(n-1)\tau$. The output pulse level during the time interval $(n-1)\tau \le t < n\tau$ can be calculated, the result is

$$V_{out} = V_1^-(n-1) = V_{in}\left[R_0 + (1-R_0^2)\frac{1-(R_0 p)^{n-1}}{1-R_0 p}\, p \right]. \qquad (5)$$

Indeed, this is the essence of passive pulse compression system. The maximum power gain is limited. Using Eq. (5), the maximum power gain as $n\to\infty$ is,

$$Maximum\ Power\ Gain = \frac{17}{p^2} - 8 - \frac{12\sqrt{2(1-p^2)}}{p^2}, \qquad (6)$$

which occurs at $R_0 = \frac{1}{p} - \frac{\sqrt{8(1-p^2)}}{4p}$. Clearly the maximum power gain is limited to 9 as $p\to 1$. Furthermore, this maximum is greatly affected by the losses in the delay line; for example, the gain is limited to 7.46 if the line has a 1% round trip power losses.

To discharge the line, one can keep the input signal at a constant level during the time interval $0 \le t < n\ \tau$ but switching the iris reflection coefficient to zero so that all the energy stored in the line is dumped out. In this case,

$$V_{out} = \frac{1-(R_0 p)^n}{1-R_0 p}(1-R_0^2)^{1/2}\, pV_{in}. \qquad (8)$$

This is a very important application of an active pulse compression system; because we do not require the change of the phase of the input pulse it enables us to use this system with an oscillator like sources.

To reduce the burden on the switch one can reverse the phase together with changing the iris reflection coefficient. In this case all the energy can still be dumped out of the line, but the iris reflection coefficient need not be reduced completely to zero. This reflection coefficient during the discharging phase R_d is greater than zero and the switch need only change the iris between R_0 and R_d. In this case the output reduces to

$$V_{out} = R_d\left[1 + \left(\frac{1-(R_0 p)^{n-1}}{1-R_0 p} \right)^2 (1-R_0^2)\, p^2 \right] V_{in}; \qquad (9)$$

where the required R_d to discharge the line completely is given by

$$R_d = \cos\left[\tan^{-1}\left(\frac{1-(R_0 p)^{n-1}}{1-R_0 p}(1-R_0^2)^{1/2}\, p \right) \right]. \qquad (10)$$

The compressed pulse takes place in the interval $(n-1)\tau \le t < n\tau$. The optimum value of R_0 is such that it fills the system with maximum possible amount of energy in the time interval $(n-1)\tau$.

Unlike the passive systems, the maximum power gain has no intrinsic limit. It is only limited by the compression ratio n and the amount of losses in the storage line. For lossless systems with $n>12$, the compression efficiency is flat at 81.5%, which means that the power gain is 81.5% of n even with the compression ratio goes to infinity. For an active system with 8% round trip power loss and the compression ratio of 20, the optimized compression gain is 9.41 if the input phase can be reversed. In this case the gain is already higher than 9, which is the intrinsic limit of the passive system. The

passive system with same compression ratio and round trip loss will yield a gain of 5.18; the gain can be enhanced to 5.91, assuming that the round trip loss can be reduced to 4% by removing the switch.

III. THE SWITCHABLE IRIS MODULE

As described above, the active pulse compression system requires a switchable iris with certain coupling coefficients at charging and discharging phases. The optimized coefficients are functions of many variables such as compression ratio, losses in the delay line and losses at the iris. A tunable iris module was then designed to match coupling coefficients of the active window to desirable values at both *on* and *off* states.

The module is composed of a Tee junction with the an active window and a movable short plane connected to the 3rd port, as shown in Fig. 2 and Fig. 3. The coupling coefficients of the module are determined by the reflection phase in the 3rd arm. A more detailed derivation of this relationship can be found in [10]. Here we only give some useful equations and derive related results for our design.

For a lossless symmetric Tee junction, the S-matrix can be written in the form

$$S=\begin{pmatrix} \frac{e^{j\phi}-\cos\theta}{2}e^{j\alpha} & \frac{-e^{j\phi}-\cos\theta}{2}e^{j\alpha} & \frac{\sin\theta}{\sqrt{2}}e^{j\alpha/2} \\ \frac{-e^{j\phi}-\cos\theta}{2}e^{j\alpha} & \frac{e^{j\phi}-\cos\theta}{2}e^{j\alpha} & \frac{\sin\theta}{\sqrt{2}}e^{j\alpha/2} \\ \frac{\sin\theta}{\sqrt{2}}e^{j\alpha/2} & \frac{\sin\theta}{\sqrt{2}}e^{j\alpha/2} & \cos\theta \end{pmatrix}; \qquad (11)$$

where the parameters ϕ and θ determine the coupling between the ports of the tee, while α is the parameter related to the location of reference planes of the ports.

When the 3rd port of the Tee is shorted as shown in Fig.2, the resultant two-port S-matrix can be expressed as:

$$\hat{S}=\begin{pmatrix} \cos\frac{\zeta-\phi}{2}e^{j(\frac{\zeta+\phi}{2}+\alpha)} & j\sin\frac{\zeta-\phi}{2}e^{j(\frac{\zeta+\phi}{2}+\alpha)} \\ j\sin\frac{\zeta-\phi}{2}e^{j(\frac{\zeta+\phi}{2}+\alpha)} & \frac{\zeta-\phi}{2}e^{j(\frac{\zeta+\phi}{2}+\alpha)} \end{pmatrix}; \qquad (12)$$

where the phase ζ is defined as,

$$e^{j\zeta}=\frac{-\cos\theta+e^{j\Psi}}{1-\cos\theta e^{j\Psi}}. \qquad (13)$$

When $\cos\theta\neq\pm1$, i.e.; the third port is not decoupled from the three-port network, or the 3rd arm is not fully blocked, a change in Ψ will result in a change in ζ. The amplitude of the normalized voltage in the 3rd arm is then given by:

$$\left|V_3^+\right|^2=\left|V_3^-\right|^2=\frac{1}{2}\frac{(1+2\cos\theta\cos\zeta+\cos^2\theta)}{\sin^2\theta}\left|V_1^++V_2^+\right|^2. \qquad (14)$$

The maximum electric field of the standing wave in the 3rd arm E_{max} at phase ξ from the short plane is given by:

$$E_{\max}=2\left|V_3^-\right|\left|\sin\xi\right|\Big/\sqrt{AG}\ , \qquad (16)$$

$$E_{\max} = 2\sqrt{\frac{(1+2\cos\theta\cos\zeta+\cos^2\theta)}{2\sin^2\theta}}\left|\sin\xi\right|\sqrt{\frac{P_{in}Z_g}{AG}}\ ; \quad (17)$$

where A is the area of cross-section of waveguide and G is the geometric factor determined by the shape of the cross-section and the mode. P_{in} is the equivalent power $\left|V_1^+ + V_2^+\right|^2 / Z_g$ and Z_g is the waveguide impedance.

When the active window is *off*, the loss P_{loff} dissipated in the active window is proportional to $\left|E_{window}\right|^2$. The *on* state loss is $P_{lon} = 4\left|V_3^+\right|^2 \frac{R_s}{Z_g}$.

In the extreme case of high compression ratio and the use of an oscillator like source, $\cos\zeta/2$ needs to be changed from near 1 to a value near 0 during switching. To minimize the voltage in the 3rd arm in both cases, a reasonable choice for $\cos\theta$ should be near 0, i.e. the third-port is matched and the power splits equally between the other two ports for an incident wave on that port.

When the active window is turned on, it acts as a short plane and the phase of the reflected signal from the third-port changes. Hence, the coupling coefficients relating the remaining two ports are switched. These coefficients depend on the location of the movable short, which determines the coupling in the *off* state, and the location of the active window, which determines the coupling in the *on* state.

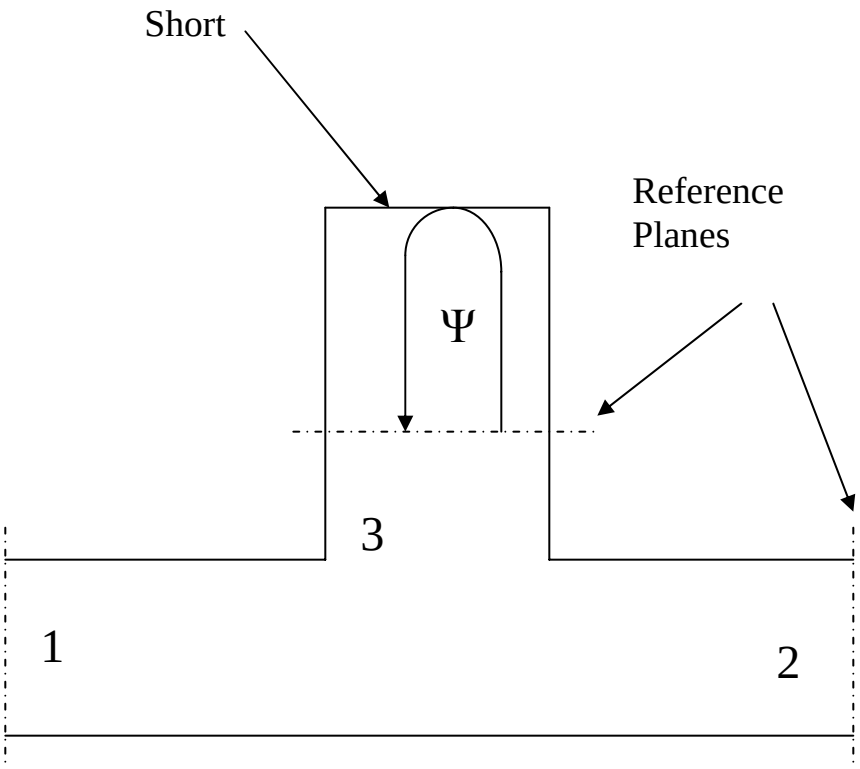

Figure 2. Symmetric Tee-junction with the symmetrical arm shorted.

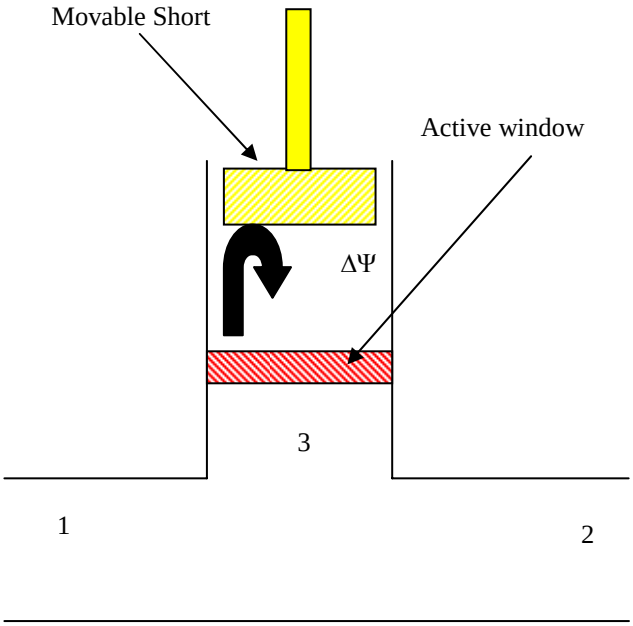

Figure 3. The tunable switch module.

A low-loss circular waveguide Tee junction has been specially designed and machined for our test setup. This Tee is composed of a TE_{20} mode rectangular Tee and 3 circular-to-rectangular mode converters [11], with S_{33}=0. Fig. 4 shows the model assembly of the circular waveguide Tee. The rectangular Tee is an E-plane Tee, hence the Tee geometry does not affect the mode index.

The circular-to-rectangular taper comprises three sections. The first taper takes the rectangular shaped waveguide into an approximately elliptical shaped waveguide. Both guides are overmoded, and several modes can propagate. However, the modes that are excited by the incident TE_{20} mode have to respect both geometrical symmetries and the incident mode symmetries. The dimensions of the rectangular and the elliptical-like waveguide allow only two such modes to propagate, at the elliptical-like waveguide we call these two modes M_1 and M_2. The second section is a straight waveguide with the elliptical-like cross section. This is used to change the relative phase between M_1 and M_2. The third section is a taper between the elliptical-like waveguide and circular waveguide. Again, the circular waveguide is overmoded, with several modes that can propagate. However, only two modes that respect the excitation symmetries of M_1 and M_2 and the geometrical symmetries of the taper can propagate in the circular waveguide, namely the TE_{01} mode and the TE_{21} mode. The first taper and the third and final taper are matched with respect to M_1 and M_2 in the sense that the relative amplitudes of M_1 and M_2 are the same for either excitation by an incident TE_{20} from the rectangular port or TE_{01} from the circular port. Hence, by adjusting the phase relation through the middle section the TE_{01} mode is reconstructed perfectly at the circular port.

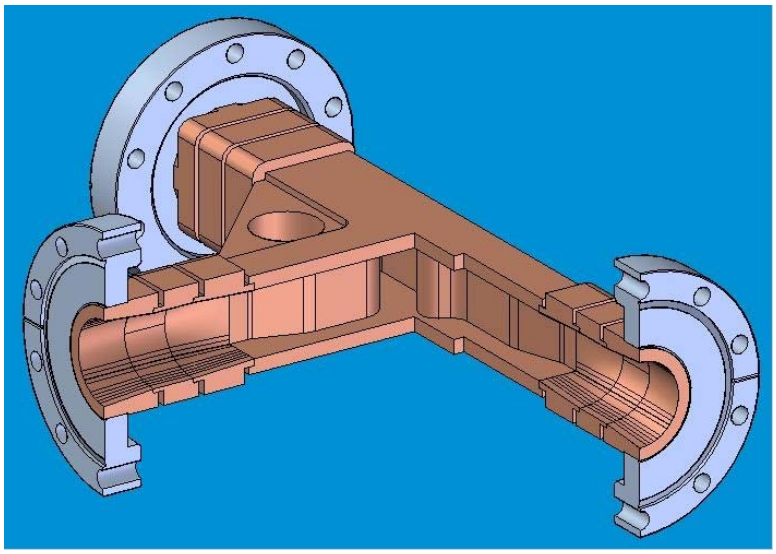

Figure.4. Model Assembly of the Circular Waveguide Tee

IV. PHYSICS AND DESIGN OF THE ACTIVE SILICON WINDOW

The authors have developed a newer version of the active switch window working in a circular waveguide, which is in common with the older Tamura design. However, we have chosen the planar structure PIN diodes, with both P and N doping on the front surface of the silicon window. The cross-section of the diode is shown in Fig. 6. The planar structure makes shorter intrinsic region length possible, so the switching speed can be enhanced. When the planar diodes turn on, the injected carriers concentrate near the top surface of the silicon wafer, which can help reduce the RF losses. The switch stays off during the charging phase of the pulse compression system and turns on to discharge the pulse, which is opposite to the older Tantawi and Tamura design and helps to reduce losses in the charging phase and enhance switching speed.

This switch also works under TE_{01} mode, as illustrated in Fig. 5 below. Since both P and N doping regions are on the same side and the number of diodes is large, the biasing needs some special design. The positive biasing of each diode is provided by a metal line from the edge of the wafer. The metal lines providing negative biasing are extended out from a metal ring in the center, and the metal ring is connected to the outside by 24 metal lines instead of several hundred. The diodes only cover a ring between the waveguide wall and metal ring.

The metal ring's width and radius can be adjusted so that the window can be matched when the switch is off. This is very helpful in reducing the maximum field in the 3rd arm during the charging phase, and it also reduces the losses. More interesting is that this ring also helps the reflection of the RF signal when the switch is on; hence, it reduces the required density of injected-carriers. The diodes only need to cover a smaller area in the waveguide cross section where the TE_{01} mode peak field is located.

At an operating frequency of 11.424 GHz, our current design uses a waveguide with 3.3cm diameter and the diode ring is only 2.5mm wide, covering only 20% of the waveguide cross section. With 3.3cm diameter, the cut-off frequency of the waveguide is very close to the working frequency. This reduces the required amount of carriers and

helps to enhance switching speed, but will compromise the power handling capability and the *off* state RF losses a little bit.

Simulation with HFSS [12] shows that when the diodes are *off*, the window has 1.6% losses and 97% transmission coefficient. This assumes a 500μm thick silicon wafer with a 10KΩcm resistivity. When 100K Ωcm silicon wafer is used, the loss is reduced to 0.7% and transmission coefficient is increased to 98%. Without the inner metal ring on the wafer, the reflection will be more than 80%. When diodes are on, eventually a carrier layer with 50 μm thickness and a density of $5\times10^{16}/cm^3$ is formed. This layer and the metal ring result in a transmission of less than 1% and power losses of about 10%. To achieve this carrier density, the switch needs about 70μC of evenly distributed carriers. The simulation does not include the radial metal lines and the doped region of the diodes. Since the dopants have a Gaussian like distribution in the doped region, the tail of the distribution will cause some more RF loss.

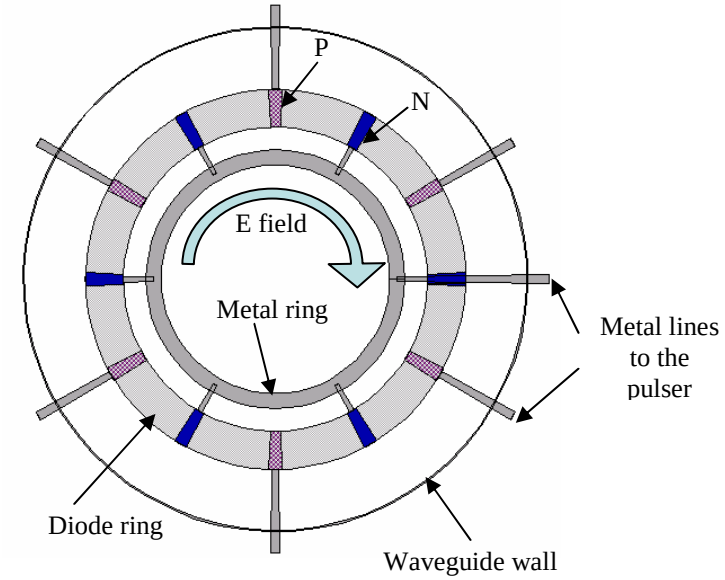

Figure.5 Schematic view of the silicon window

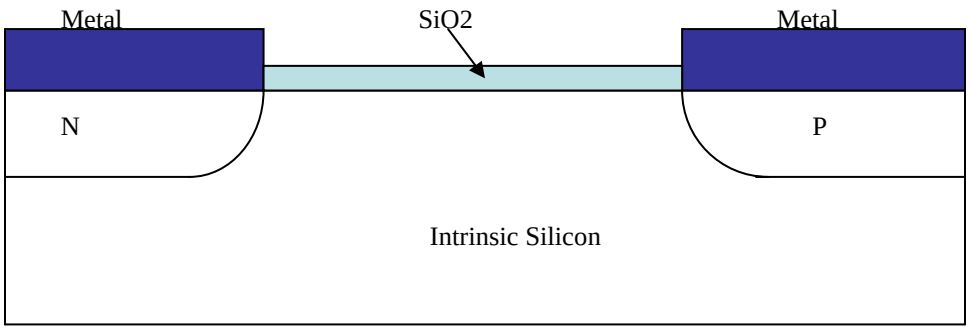

Figure. 6 Cross-section view of one PIN diode (not to scale)

When the diode is forward biased, carriers are injected from the contacts and drift/diffuse into the intrinsic region. The amount of injected carriers equals to the charges provided by the biasing circuit. If the carrier lifetime is significantly longer than

the switching time, the speed of the switch will essentially depends on the available current from the biasing circuit and the amount of the required carriers.

Because of the non-uniform distribution of the carriers, the actual amount of carriers needed is significantly larger than the above estimated value. To minimize non-uniformity, the length of the diode (distance between P and N region) should be less than one or two diffusion lengths. One-dimension diode with two large parallel plate electrodes can also enhance uniformity, but it's very hard to integrate such a one dimensional diode into this switch, and the large doping area of the diodes will cause higher losses.

We have simulated the time response of the diodes with the Medici code [15]. The dopant profiles of the devices used in Medici simulation were imported from the result of process simulation with TSupreme [16]. The actual process was optimized based on the simulation results. For planar structure diodes with 60μm length, which are connected in parallel, simulation shows that the average carrier density of the top 50 μm layer at center of the diodes will rise to $5\times10^{16}/cm^3$ after about 200 μC of charges injected. With a current source providing 1 kA pulse with 50ns rise time, the switch can be turned on in 250ns. The carrier lifetime is assumed to be > 100 μs.

Carriers can also be generated by impact ionization. When the electric filed is above a certain value, the carriers gain enough energy and will excite electron-hole pairs in the path they travel. The number of electron-hole pairs generated by a carrier per unit distance it travels is defined as the ionization rate, which varies approximately exponentially with the electric field. When the field is higher than 300KV/cm, the ionization rate is high enough to breakdown the silicon. Such field can be achieved by applying high voltage reverse bias on the diode, or by the high power RF field. So the switch can work faster with high power RF.

The reverse bias impact ionization could be another possible efficient way to create large amount of carriers in short time. Although contact injection usually only needs 1V of voltage to create carriers, the high current needed for fast injection creates huge voltage drop on the inductance and resistance in the circuit. In our experiments, we need between 500V and 1000V for the forward bias. The reverse bias voltage needed to breakdown the diode in our design is not much higher than 1kV, but the required current integral could be much less. The breakdown of diodes can be faster and more uniform if a low power laser or flash light is used to generate some "seed" carrier.

Figure 7. Fabricated Active Window

We have made such a switch; it is shown in Fig 7. The fabrication of the switch was completed at the Stanford Nanofabrication Facility, with CMOS compatible process. Several round of fabrication have been completed, and the design was improved each round based on testing results. The switch was built on a Floatzone silicon wafer with 90K Ωcm resistivity and 500 μm thickness. The parameters of the anneal procedure was chosen to compromise carrier lifetime and the loss in the diffusive doped region.

V. EXPERIMENTAL RESULTS

We have characterized these switches with both network analyzer measurements and active switching tests; we performed the tests under the one-pass setup shown in Fig. 8 as well as the module setup with the switch attached to the circular Tee and a movable short shown in Fig. 9. After that, we attached the switch at the end of a 375 ns resonant delay-line and tested the active pulse compression system. The setup of the active pulse compression experiment is shown in Fig. 12.

A. Characterization Experiments

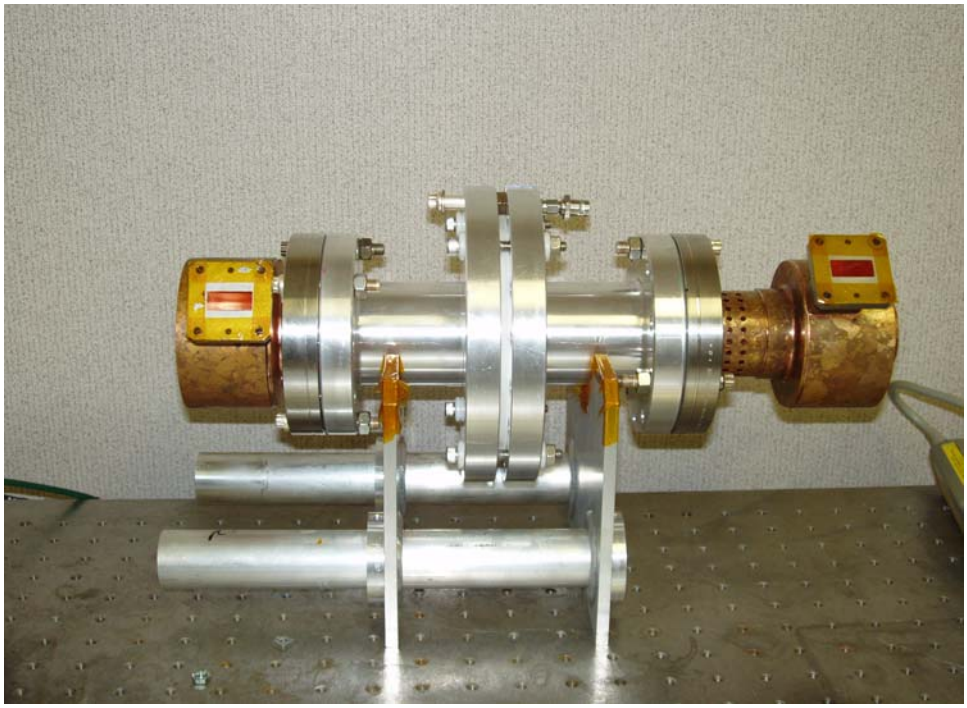

Figure 8. Holder of the Active Window

In the one-pass network analyzer characterization, we have measured S_{12}=0.90 and S_{11}=0.35 with 6.5% loss, including about 2% losses over the mode converter. Part of the discrepancy between the simulation and the measurement may come from a 5mm gap in the wafer holder. The gap might be large enough to leak RF out. A new holder with smaller gap is under construction at the time of writing this paper. The radial metal lines, the diode doping, and the variation in wafer thickness will also increase the reflection and/or losses. The losses from the doped region have been improved significantly by reducing both implantation dose and annealing time.

Fig. 10 shows the S-matrix as a function of the position of the short plane in the back of the switch, with the *on*-state reflection coefficient has been tuned to about 0.38. It shows that the reflection coefficient of *off* state can be tuned successfully with moderate losses.

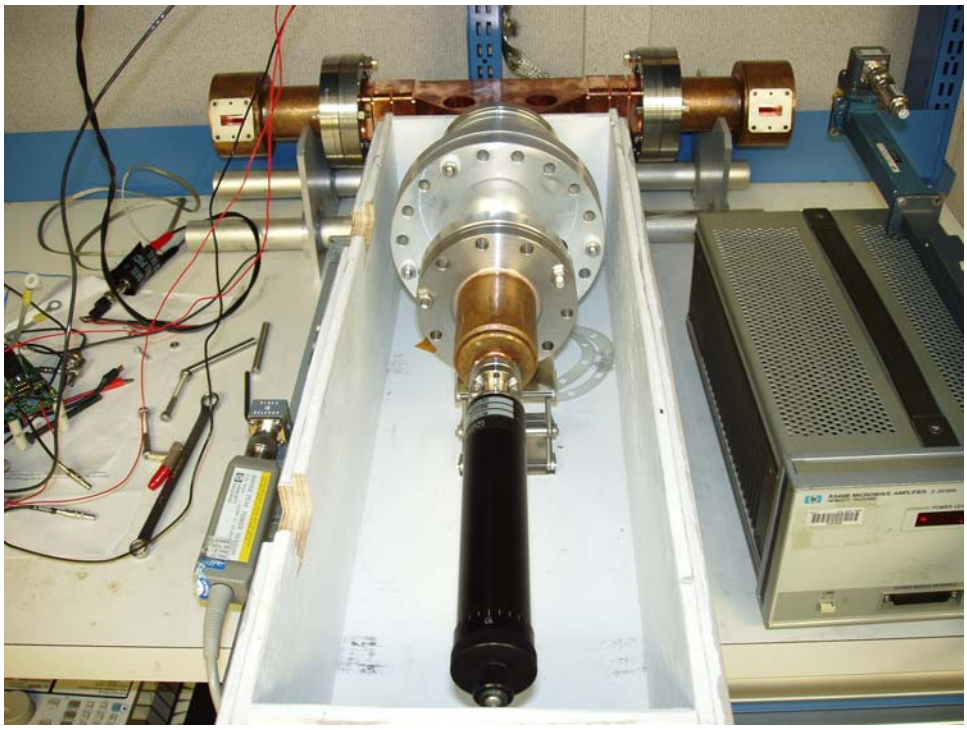

Figure 9. The Switch Module with Movable Short and Circular Waveguide Tee.

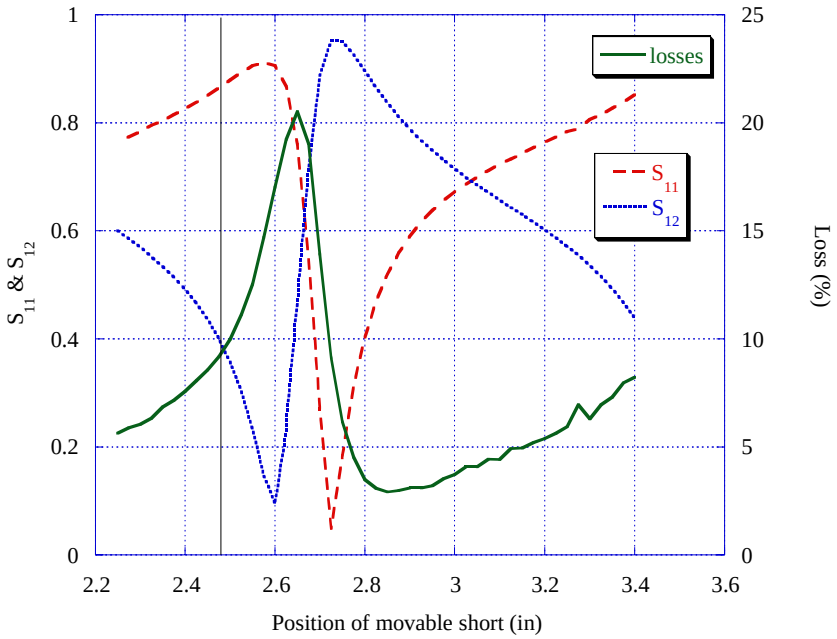

Figure 10. S Matrix and loss of the switch module

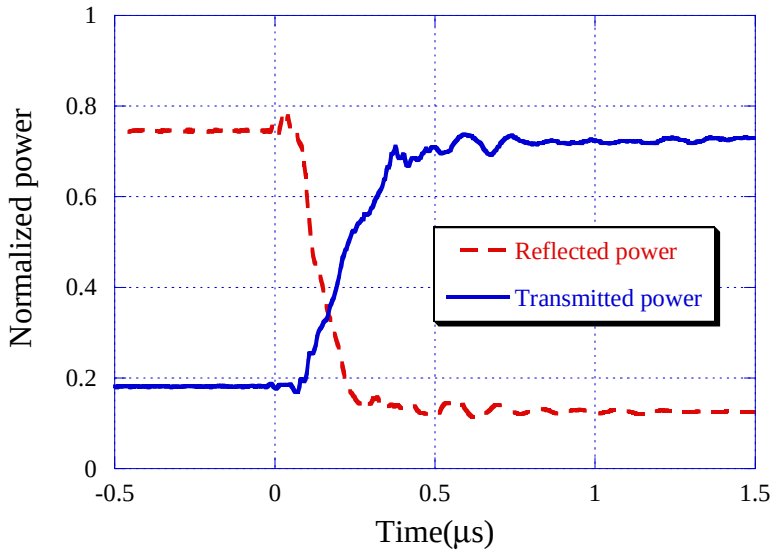

Fig. 11 Active switching test with switch module

Active switching tests have been performed both with one-pass setup and the module setup. Peak RF power analyzer was used to measure the input and the transmitted/reflected power through directional couplers. The switch is powered by an IGBT circuit, using two IXYS EVDD408 evaluation boards driving 6 IRGPS60B120KD IGBT transistors. The current output of this circuit is monitored by one 0.2Ω low inductance resistor on each board. With 700 V over the IGBT and the load, the current output can rise to 600 A in about 40 ns, and then rise to 1400A in 300 ns. If the serial resistance and inductance in the circuit can be reduced further, i.e., the current monitor resistor is removed, similar current output can be generated with voltage lower than 500V.

Fig. 11 shows the time response of the switch module. The switching time is about 300 ns. The *on* state losses are measured at about 15%. A 300 ns switching time and similar on state losses has also been observed in the one-pass setup.

B. Active Pulse Compression Experiment

In the setup of the active pulse compression as shown in Fig. 12, port 2 of the switch module is attached to a 375ns resonant delay line, and the port 1 is connected to the RF input. The switch is driven by 700V 1400A pulses with 250ns duration. The optimized test results are shown in Fig. 13 and 14. In all the tests, input pulse width is 20 times longer that output pulse width; i.e., a compression ratio of 20. For a system which cannot flip the phase of the RF input, the switch turns on when the input turns off. Almost 6 times power gain has been observed, compared to a theoretical gain of 2 times for a passive compression system without phase flipping, given the losses of our delay lines.

For a system which can flip the phase of the RF input before the last input bin, the switch turns on at the same time of the phase flip. The active system has achieved almost

8 times compression gain to be compared with the gain of 5 achieved by the passive system.

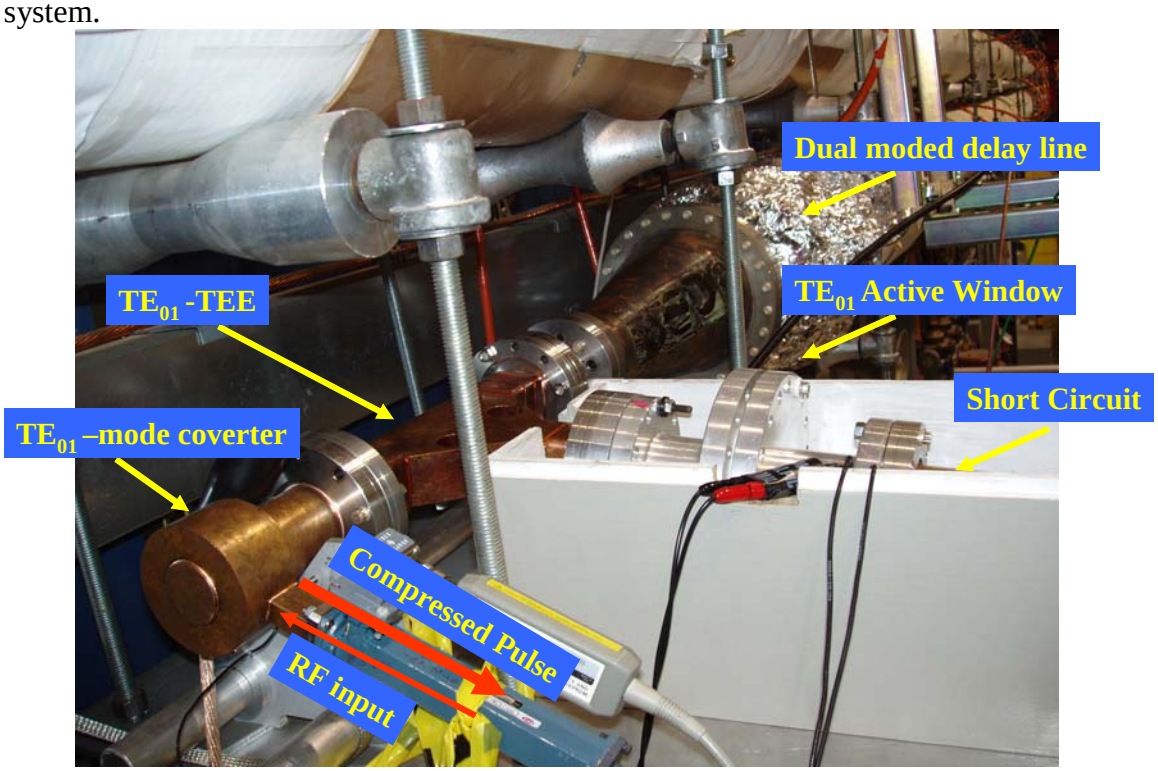

Figure. 12. The Active Pulse Compression Experiment Setup

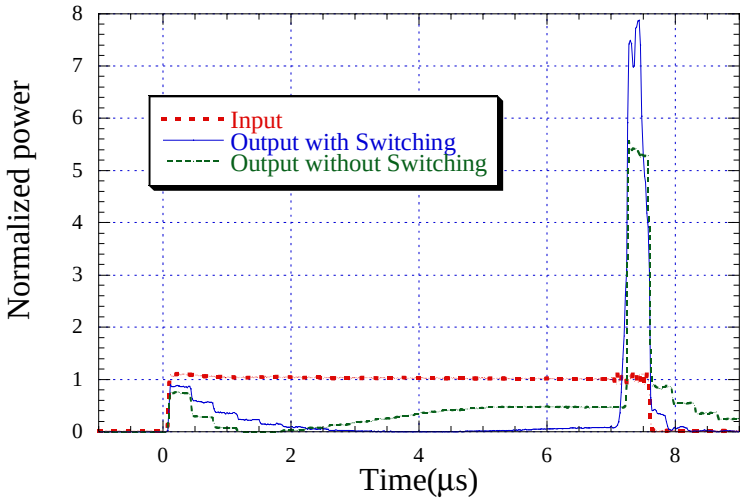

Figure 13. Active Pulse Compression Test with Input Phase flipped

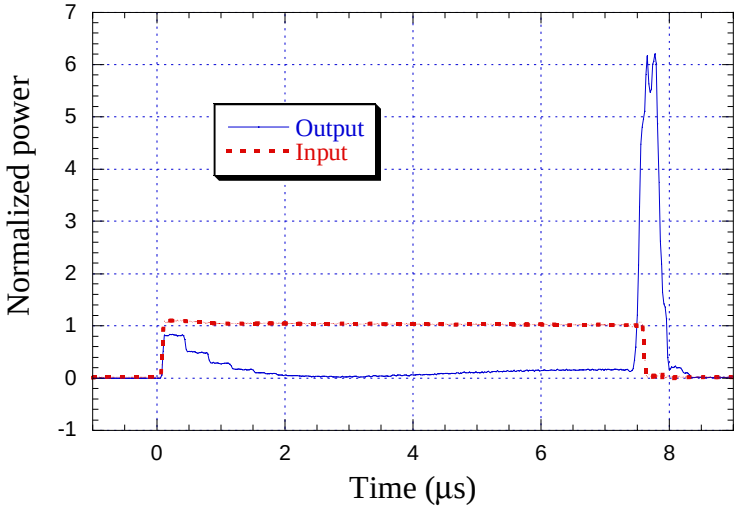

Figure 14. Active Pulse Compression Test without Input Phase flipped

VI. SUMMARY

We have reviewed the theory of active pulse compression system. We also reviewed the theoretical foundations for the implementation of ultra-high-power RF switch, the key component for this system. We showed an implementation for such a switch using a novel overmoded circular TE_{01} mode three-port network. We presented the design and implementation of an array of PIN diodes spatially combined into the TE_{01} mode circular waveguide. The active window which comprises the array of PIN diodes has two fundamental novel features that enables it to be fast and reduces its losses. First, the diodes are contained on the surface of the silicon wafers and confined to a small ring-shaped region at the peak of the electric field radius. This reduces the total amount of charge needed to switch the reflectivity of the window. Second, the matching of the window at the *off* state is done by a metallization ring, which serves also as parallel feed for the biasing of the diodes. We demonstrated the use of such a device in a pulse compression system with substantially improved gain over the passive system. We showed also, for the first time the possibility of using such a system to compress the output of an oscillator like source. This was not possible before.

A high power experiment needs to be completed in the future, which will determine the power handling capacity of this switch and the time response under high power RF field. With the assistance of high power RF field, the switching speed is expected to be faster than the low power test results.

To make the switch more practical for pulse compression application, the switching speed needs to be enhanced further. For the current version of our switches, the speed can be enhanced with higher injection current. However, the maximum current is limited by the serial impedance in the circuit. We only expect a couple times of switching speed increase with this approach. Another possible approach to explore is to generate carriers with impact ionization by breaking down the diodes with reverse bias. This approach may

reduce the required current significantly but only requires a voltage not much higher than 1kV with the same switches in the current experiments. With the assistance of optical carrier injection, it is possible to enhance the switching speed by one order of magnitude, and make it suitable for RF pulse compression systems with shorter output width.

References:

1. Z. D. Farkas et al, "SLED: A Method for Doubling SLAC's Energy", *Proceeding of 9th Int. Conf. on High Energy Accelerators*, Stanford, California, 1974.
2. Z. D. Farkas, "Binary Peak Power Multiplier and its Application to Linear Accelerator Design", *IEEE Transactions on Microwave Theory and Techniques*, Vol. 34, No. 10, October 1986
3. P.B Wilson et al, "SLED-II: A New method of RF pulse compression", *Proceedings of the 1990 Linear Accelerator Conf.*, Albuquerque, New Mexico, 1990
4. A.Fiebig et al, "A SLED type pulse compressor with rectangular pulse shape", *Proceedings of the 2nd European Particle Accelerator Conference*, Nice, France, 1990.
5. S. G. Tantawi et al, "Active RF pulse compression using switched resonant delay lines", *Nuclear Instruments & Methods in Physic Research, Section A*, Vol.370, pp. 297-302, 1996.
6. Tantawi, S.; "Overmoded high-power RF magnetic switches and circulators", *Proceedings of the 2001 Particle Accelerator Conference*, Chicago, Illinois, 2001.
7. Yakovlev et al, "High Power Ferroelectric Switches at Centimeter and Millimeter Wave Lengths", *Proceedings of the 2005 Particle Accelerator Conference*, Knoxville, Tennessee, 2005
8. A. L. Vikharev et al, "Experiments on Active RF Pulse Compressors Using Plasma Switches", *Proceedings of the 7th Workshop on High Energy Density and High Power RF*, Kalamata, Greece, 2005
9. S. G. Tantawi et al, "Active high-power RF pulse compression using optically switched resonant delay lines", *IEEE Transactions on Microwave Theory and Techniques*, Vol. 45, Issue. 8, pp1486 – 1492, 1997
10. F. Tamura and S. G. Tantawi, "Development of high power X-band semiconductor microwave switch for pulse compression systems of future linear colliders", *Physical Review Special Topics - Accelerators and Beams*, Volume 5, 062001 (2002)
11. Sami G. Tantawi et al, "High-power multimode X-band RF pulse compression system for future linear colliders", *Physical Review Special Topics - Accelerators and Beams*, Volume 8, 042002 (Issue 4 – April 2005) [19 pages], see also, V. A. Dolgashev et al, "Design of a compact, multi-megawatt, circular TE(01) mode converter", *Proceedings of the 7th Workshop on High Energy Density and High Power RF*, Kalamata, Greece, 2005
12. Ansoft Corporation, HFSS V9.2, http://ansoft.com .
13. K. Mortenson et al, "A Review of Bulk Semiconductor Microwave Control Components", *Proceedings of The IEEE*, Vol. 59, No. 8, 1971
14. K. Mortenson et al, "Microwave Silicon Windows for High-Power Broad-Band Switching Applications", *IEEE Journal of Solid-State Circuits*, Vol. SC-4, No. 6, 1969
15. Synopsys Inc., Medici Two-Dimensional Device Simulation Program, Version 4.0
16. Synopsys Inc., TSUPREM-4 Two-Dimensional Process Simulation Program, Version 4.0
17. M. Sze, "Physics of Semiconductor Devices", 2nd Ed, John Wiley & Sons, 1981.